



# Current Problems in Diagnostic Radiology

journal homepage: [www.cprjournal.com](http://www.cprjournal.com)



## Comparative Evaluation of Brain Tuberculosis and Metastases Using Combined Analysis of Arterial Spin Labeling Perfusion and Diffusion Tensor Imaging

Neetu Soni, MD, DNB<sup>a,\*</sup>, Sunil Kumar, MD<sup>b</sup>, Karthika Srintharan, MD<sup>b</sup>, Prabhakar Mishra<sup>c</sup>, Nishant Gupta, MD<sup>d</sup>, Girish Bathla, DMRD, MMed, FRCR<sup>e</sup>, Jyantee kalita, MD, DM<sup>f</sup>, Sanjay Behari, MS, MCh<sup>g</sup>

<sup>a</sup> Neuroradiology Department, UIHC, Iowa city, IA

<sup>b</sup> Radiology Department, SGPGIMS, Lucknow, Uttar Pradesh, India

<sup>c</sup> Department of Biostatistics and Health Informatics, SGPGIMS, Lucknow, Uttar Pradesh, India

<sup>d</sup> Columbia University Medical Center, New York, NY

<sup>e</sup> Radiology Department, UIHC, Iowa city, IA

<sup>f</sup> Department of Neurology, SGPGIMS, Lucknow, Uttar Pradesh, India

<sup>g</sup> Department of Neurosurgery, SGPGIMS, Lucknow, Uttar Pradesh, India

### ABSTRACT

**Purpose:** To differentiate intra-axial tuberculomas (TB) from metastases based on quantitative differences in the perfusion and diffusion indices of lesion and perilesional edema using arterial spin labeling (ASL) and diffusion tensor imaging (DTI) techniques.

**Materials and methods:** This prospective study included newly diagnosed untreated 12 patients of TB and 13 of metastases who underwent routine magnetic resonance imaging including DTI and ASL sequences. A region of interest analysis was performed and cerebral blood flow (CBF) values of lesion (L), perilesional edema (PE), and normal contralateral white matter (CWM) were calculated. To account for individual patient variation CBF values were normalized (n) to CWM to obtain the nCBFL and nCBFPE ratios. Similarly, DTI data was processed to obtain fractional anisotropy (FA), mean diffusivity, radial diffusivity, and axial diffusivity values from the lesion and PE.

**Results:** Metastatic lesions revealed statistically significant ( $p = 0.001$ ) high values of median nCBFL than TB whereas the difference in the median nCBFPE was not statistically significant ( $p = 0.174$ ). TB showed higher median FAL compared to metastases ( $p = 0.031$ ) while no statistically significant difference was found in mean values of other diffusion parameters such as mean diffusivity, radial diffusivity and axial diffusivity. Analysis by the receiver operating characteristic curve method revealed a cut-off value of  $\geq 2.865$  for nCBFL (Sensitivity = 0.85, Specificity = 0.84, positive predictive value (PPV) = 0.85, Negative predictive value (NPV) = 0.83) and  $\leq 0.073$  for FAL (Sensitivity = 0.77, Specificity = 0.58, PPV = 0.67, NPV = 0.70) in differentiating metastases from TB.

**Conclusion:** Combined analysis of noncontrast ASL perfusion and DTI technique may markedly benefit in differentiation of TB from metastases.

© 2018 Elsevier Inc. All rights reserved.

### Introduction

Central nervous system (CNS) tuberculosis (TB) is one of the major causes of morbidity and mortality in developing countries. TB is also at a rising trend in the developed countries especially in underlying human immunodeficiency virus infection. CNS TB accounts for about 1% of all TB infections, causing neurological deficits which mandates early diagnosis and treatment to avoid permanent damage. Intracranial tuberculomas are classically conglomerated lesions composed of a central caseation necrosis surrounded by a zone of fibroblasts, Langhans giant cells, and

lymphocytes.<sup>1,2</sup> It often presents as a diagnostic challenge and may resemble many other infectious and noninfectious conditions such as metastasis, lymphoma, gliomas, abscess, demyelinating lesions, and other infective granulomas. Metastatic lesions are usually multiple, located near the gray-white matter junction and often with a known background history of systemic malignancy. Approximately 30% of metastatic lesions can manifest as a single intracranial lesion and in some cases as the initial clinical presentation of systemic malignancy.<sup>3</sup> Both tuberculomas and metastases are among the most common differential diagnosis of ring enhancing lesions. It is essential to differentiate between tuberculoma and metastasis to guide the proper management and prognosis. On conventional magnetic resonance imaging (MRI), both do have some specific imaging features, however none is found to be unique in distinguishing these as both can present as single or multiple ring or nodular-enhancing lesions with perilesional white matter edema. Even on Magnetic resonance spectroscopy (MRS), both lesions show lipid peaks and the spectra may not be useful in presence of small lesions,

Source of support: NIL.

Presentation at a meeting: Not done.

Conflicting of interest: None.

Permissions: Institutional review board and Ethics committee.

\*Reprint requests: Neetu Soni, MD, DNB, FRCR, Neuroradiology Department, UIHC, Iowa city, IA, 52246.

E-mail address: [neetu\\_soni06@yahoo.co.in](mailto:neetu_soni06@yahoo.co.in) (N. Soni).

<https://doi.org/10.1067/j.cpradiol.2018.09.003>

0363-0188/© 2018 Elsevier Inc. All rights reserved.

intralesional calcifications, and hemorrhage.<sup>4,5</sup> Guided biopsy is done in a few cases for the confirmation; however, in most of the cases, a trial of anti tubercular treatment (ATT) is given which delays in management for those who harbor metastasis. Recently, advanced MRI techniques such as perfusion and diffusion tensor imaging have been investigated in many conditions to assess their utility.

Arterial spin labeling (ASL) is a nonionizing and noninvasive MR perfusion technique measures tissue perfusion (blood flow) by using magnetically labeled arterial blood water protons as an endogenous tracer. These benefits make ASL very suitable for perfusion studies in healthy individuals, patients with renal insufficiency and for repetitive follow-ups. In brain lesion evaluation, dynamic susceptibility contrast (DSC) is favoured over ASL because of rapid data acquisition and routine contrast use. However, cerebral blood flow (CBF) quantification in DSC is affected by T1 and T2 effects of blood-brain barrier (BBB) disruption and susceptibility artifacts which are less common with ASL. Multiple prior studies have shown a very strong correlation between ASL and DSC-MRI derived perfusion parameters for evaluation of brain tumours and support the possibility that ASL can be used as an alternative to DSC-MRI.<sup>6,7</sup> Two studies have shown perfusion changes by measuring relative cerebral blood volume (CBV) and CBF in lesion and perilesional edema using DSC MRI in differentiating cerebral metastasis from tuberculoma.<sup>8,9</sup> DTI (Diffusion Tensor Imaging) provides tissue microstructural information by measuring the average and directional water diffusivity for a given voxel in terms of MD (mean diffusivity) and FA (fractional anisotropy). White matter (WM) tracts show greater degrees of anisotropy and one of the main roles of DTI is to give precise information about the involvement and integrity of the white matter tracts in the immediate region

surrounding tumors. FA is sensitive to microstructural integrity and MD sensitive to cellularity, edema, and necrosis. Axial diffusivity (AD) correlates to axonal density and decreases in axonal injury while radial diffusivity (RD) increases in WM demyelination.<sup>10–12</sup>

Understanding the perfusion and diffusion characteristics of tuberculomas and metastasis using ASL and DTI techniques respectively, may help in increase the degree of confidence of their diagnosis. In this study, we hypothesized that a combination of ASL (CBF) and DTI (FA, MD, AD and RD) parameters can assist in better differentiation of brain metastases from tuberculomas. We also assessed the feasibility of ASL as an alternative to DSC in differentiating both when needed.

## Materials and Methods

### Subject

This study protocol was approved by the ethics committee of our institution and all subjects provided written informed consent. In this prospective study (July 2015 to Dec 2016), we consecutively collected newly diagnosed 25 patients (age range of 18–65 years and M: F-8:17) of single or multiple intracranial lesions with perilesional edema detected primarily either on CT or MRI, referred for MRI to plan the clinical management. Twelve of them were diagnosed as intracranial tuberculomas (age range 18–30 years; M:F-3:9) and 13 as metastases (age range 41–50 years; M:F-5:8). Patients with brain metastases fulfilled the following conditions: (1) intracranial lesion(s) with perilesional edema, (2) presence of primary cancer, (3) no sign of tuberculosis, cryptococcosis, toxoplasmosis, or other infectious/granulomatous diseases, and (4) higher serum tumor marker if the

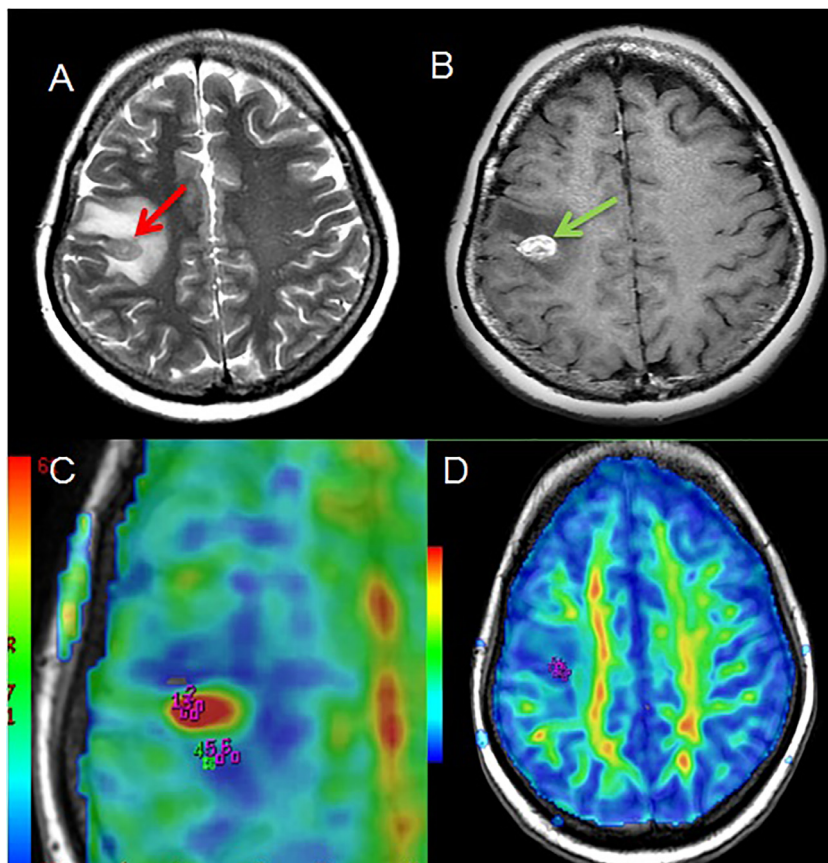


**FIG 1.** MRI images of a 48 years female with brain metastases from breast carcinoma: (A) T2-weighted imaging (T2WI) showing isointense lesion (red arrow) with perilesional edema in right frontal region (B) T1WI postcontrast showing target like peripheral enhancement (green arrow) (C) ASL perfusion map axial image showing highest normalized CBF (nCBF = 5.64) in the lesion (1,2,3 ROIs placed over region showing highest perfusion) and lower CBF (nCBFPE = 0.76) in immediate perilesional edema (4,5,6 ROIs). (D) DTI-FA map showing low FA in both lesion FAL = 0.05 and perilesional region Fractional anisotropy of perilesional edema (FAPE) = 0.13. (Color version of figure is available online.)

primary cancer secreted a specific tumor marker. Of the 13 metastatic brain lesions, 8 cases had histopathologically proven primary carcinoma breast, 4 cases of primary carcinoma lung and one rare case of parathyroid carcinoma. Patients with intra-cranial tuberculosis satisfied the following diagnostic criteria: (1) elevated DNA of tuberculosis in the CSF, (2) active tuberculosis proven from the lung imaging and sputum, (3) no evidence of primary cancer, (4) no sign of cryptococcosis, toxoplasmosis, or other infectious/granulomatous diseases in the serum test or CSF test. We excluded patients with any form of prior specific medical or surgical treatment, unknown disease, and lesion less than 0.6 cm.

### MRI Study

All patients underwent MR imaging on a 3T MR scanner (Signa HDXT, General Electric, and Milwaukee), using a 12-channel head coil. Following routine MR sequences were planned – Axial T2, T1/T2FLAIR, Diffusion weighted imaging (b value = 1000 mm<sup>2</sup>/sec) and postcontrast T1. In addition, whole brain three-dimensional pseudo-continuous ASL (3D PCASL) sequence was acquired with the hypothesis that one can differentiate between these two closely mimicking lesions without using contrast perfusion studies such as DSC.<sup>8,9</sup> 3D PCASL was acquired using following parameters: labeling

duration = 1.5 seconds, postlabeling delay = 1.5 seconds, TR = 4.4s, TE = 9.2 milliseconds, acquisition matrix = 8 arms with 512 spiraling points, NEX = 3, no. of slice = 32, FOV = 24, slice thickness = 6 mm, bandwidth = 62.50, plane = axial, scan time = 4 min with background suppression and pulse labeling plane placed just below the volume of interest. DTI was performed with following parameters (b value = 1000, matrix = 128 × 128, TR = 12.4 seconds, TE = 86.4 milliseconds, slice thickness = 3.0 mm, spacing = 0, FOV = 24, plane = axial, no. of direction = 30, NEX = 1) using same planning as ASL to co-register the DTI images with ASL images for accurate regions of interest (ROI) placement.

### Postprocessing and Data Analysis

ASL and DTI raw data were transferred to the workstation (ADW4.4, GE) for post-processing and images were analyzed using a commercial software (Functool Brain stat Software, General Electric, and Milwaukee) with automated generation of quantitative perfusion CBF maps from ASL and DTI parameters maps, such as FA, MD, RD and AD. All cases were analyzed by two neuroradiologist (N.S. with 10 years, S.K. with 35 years of experience) in consensus who were blinded to the final diagnosis. Conventional MR sequence assessed for the lesion localization, characterization and

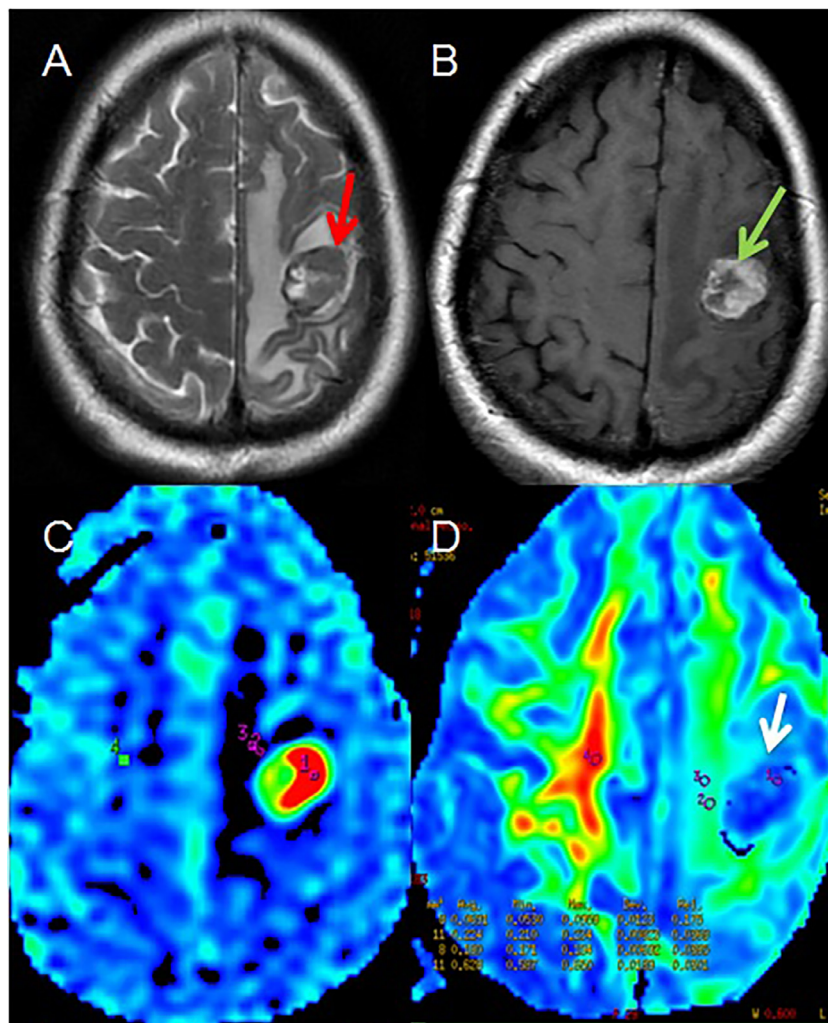


**FIG 2.** MRI images of a 58 years male with brain metastases from primary lung carcinoma: A) T2WI showing isointense lesion (red arrow) with perilesional edema in left frontal region (B) T1WI postcontrast showing peripheral and central enhancement (green arrow) (C) ASL perfusion map showing highest normalized CBF (nCBFL = 7.72) in the lesion (red region) and lower (nCBFPE = 0.87) in perilesional edema. (D) DTI-FA map showing low FA in both lesion FAL = 0.06 (white arrow) and perilesional edema FAPE = 0.15. (Color version of figure is available online.)

enhancement pattern. Lesion and perilesional edema was defined on the T2 and FLAIR images. Three circular ROIs measuring 5–10 mm<sup>2</sup> were placed in lesion (showing highest perfusion signal on CBF map) and perilesional edema (within 1 cm from the lesion) on CBF and DTI maps (Figs 1 and 2) with exclusion of necrotic, cystic and haemorrhagic areas; and average of three measurements was used for further evaluation. In case of multiple lesions, the largest lesion with maximum perfusion value was targeted for measurements. For normalization of CBF, 3 similar ROI were placed on the normal contralateral white matter (CWM). We measured the ratio of maximum CBF from lesion (nCBFL) and perilesional edema (nCBFPE) relative to that of CWM to compensate for variations in each exam. The DTI parameters from lesion and perilesional edema were not normalized to CWM.

#### Statistical Analysis

A statistical analysis was performed using statistical package for social sciences, version 23 (SPSS-23, IBM, Chicago). The normality of continuous variable's (ASL and DTI parameters) was tested using Shapiro Wilk test. For normally distributed data, mean  $\pm$  SD, while for non-normal data median, interquartiles range (IQR) was used as descriptive statistics. To compare the means when data was normally distributed, independent sample t test while for non-normal data Mann-Whitney U test was used to compare median. For comparison of ASL and DTI parameters between the metastases and tuberculosis, we used Mann-Whitney U test. Receiver operating characteristic (ROC) curve was drawn for the significant variables in the Mann-Whitney U test, to identify the cut-off value for diagnosis of brain

metastasis from tuberculosis and p value < 0.05 was considered as statistically significant.

#### Results

There was significant difference ( $p < 0.05$ ) in median nCBFL and FAL values between metastases (Figs 1 and 2) and tuberculosis (Figs 3 and 4) as shown in Table 1. However, there were no statistically significant difference ( $p > 0.05$ ) found in median of nCBFPE and means of FAPE, Mean diffusivity of the lesion (MDL), Mean diffusivity of perilesional edema (MDPE), Axial Diffusivity of lesion (ADL), Axial Diffusivity of perilesional edema (ADPE), Radial diffusivity of lesion (RDL), Radial diffusivity of perilesional edema (RDPE) (Tables 1 and 2). Area under the curve (AUC) was computed for nCBFL and FAL with corresponding diagnostic accuracy at different cutoff values. ROC curves showed the high diagnostic accuracies for nCBFL (AUC = 0.89, 95% CI = 0.74–1.00,  $p = 0.001$ ) and FAL (AUC = 0.75, 95% CI = 0.56–0.94,  $p = 0.032$ ). ROC curve method showed a cut-off value of nCBFL of 2.865 for metastasis (Sensitivity = 0.85, Specificity = 0.84, PPV = 0.85, NPV = 0.83, OA = 0.84, LR += 5.08 and LR -= 0.18) (Figure 5) and cutoff value of FAL of 0.073 (Sensitivity = 0.77, Specificity = 0.58, PPV = 0.67, NPV = 0.70, OA = 0.68, LR += 1.85 and LR -= 0.40) (Figure 6). A good AUC of nCBFL compared to the FAL (0.89 vs 0.75) indicated better test to differentiate the metastases from tuberculosis. Due to good sensitivity and specificity nCBFL (cut-off value of  $\geq 2.865$ ) and FAL (cut-off value of  $\leq 0.073$ ) can be used to differentiate between tuberculomas from metastases.

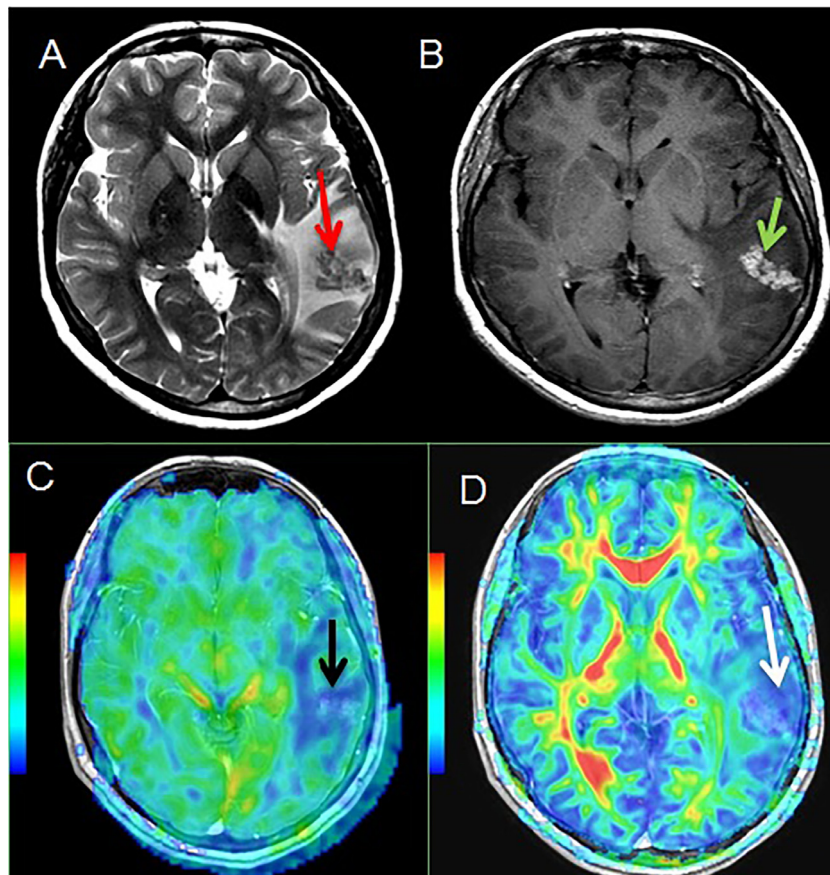


**FIG 3.** MRI images of 22 years female with tuberculoma (A) T2WI showing hypointense mass lesion (red arrow) with perilesional edema in left temporo-parietal region (B) T1WI postcontrast showing conglomerate pattern of enhancement (green arrow) (C) ASL perfusion map shows lower normalized CBF (nCBFL = 1.04) in both lesion (black arrow) and immediate perilesional edema (nCBFPE = 0.30) (D) DTI-FA map showing low FA in both lesion FAL = 0.08 (white arrow) and perilesional edema FAPE = 0.19. (Color version of figure is available online.)

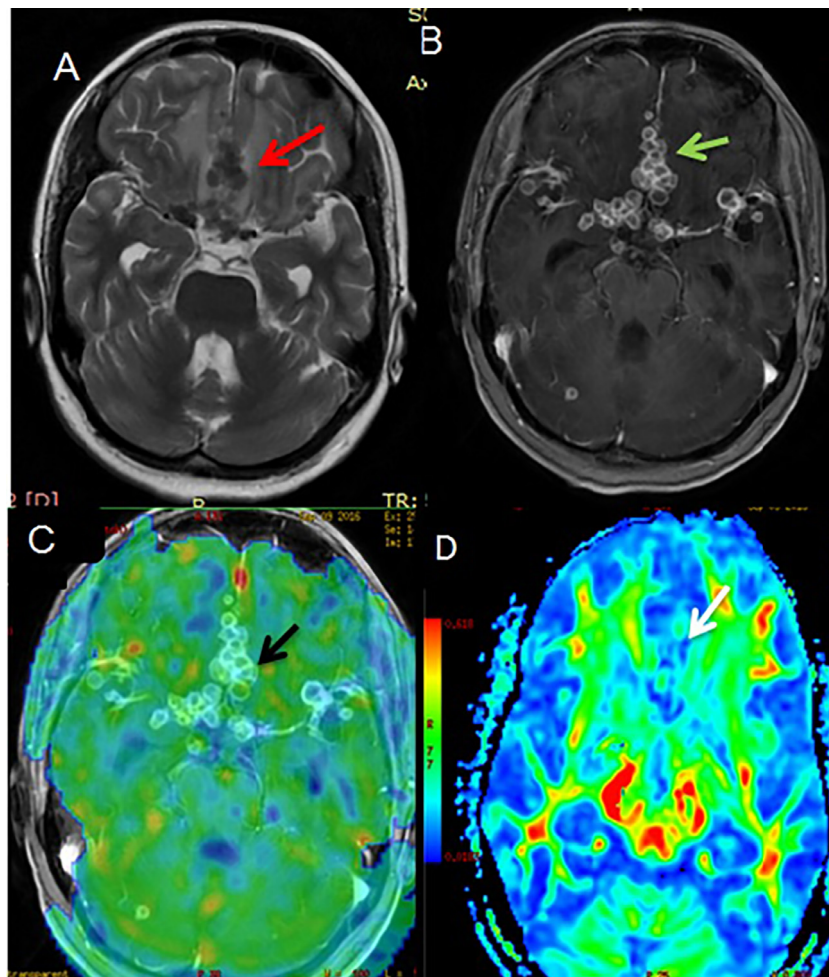


**FIG 4.** MRI images of 20 years male with tuberculoma (A) T2WI showing multiple hypointense lesions (red arrow) with perilesional edema in the basifrontal region (B) T1WI postcontrast showing conglomerate ring enhancing pattern (green arrow) (C) ASL perfusion map shows no raised CBF (nCBFL = 1.04) in both lesion (black arrow) and immediate perilesional edema (nCBFPE = 0.67) (D) DTI-FA map showing low FA in both lesion FAL = 0.08 (white arrow) and perilesional edema FAPE = 0.17. (Color version of figure is available online.)

**TABLE 1**  
nCBF and FA values in tuberculoma and metastases

Parameters	Groups	Number	Median (IQR)	p value
nCBFL	TB	12	1.78 (1.27-2.52)	0.001*
	Mets	13	5.95 (3.90-9.34)	
nCBFPE	TB	12	0.71 (0.59-0.96)	0.174*
	Mets	13	0.81 (0.70-1.08)	
FAL	TB	12	0.08 (0.06-0.11)	0.031*
	Mets	13	0.06 (0.05-0.08)	

L, lesional; PE, perilesional edema.  
The values are given as median (interquartile range).  
\*Mann-Whitney U test.

**Discussion**

In this study, the two common closely simulating intra-axial lesions, metastases, and tuberculomas were differentiated by using a combination of ASL perfusion and DTI MRI techniques based on CBF, FA, MD, AD and RD from the lesion and perilesional white matter edema. Capillary architecture in metastatic lesion resemble the organ of origin and do not possess the unique blood-brain barrier which makes them highly leaky resulting in vasogenic edema.<sup>13</sup> CNS tuberculoma can manifest as diffuse exudative leptomenigitis and focal tubercular lesions which can show variable T2 appearances and

**TABLE 2**  
FA, MD, RD and AD values in tuberculoma and metastases

Parameters	Groups	Number	Mean ± SD	p value
FAPE	TB	12	0.16	0.587**
	Mets	13	0.15	
MDL	TB	12	4.67	0.689**
	Mets	13	4.64	
MDPE	TB	12	5.07	0.566**
	Mets	13	5.01	
ADL	TB	12	4.52	0.605**
	Mets	13	4.57	
ADPE	TB	12	4.86	0.986**
	Mets	13	4.86	
RDL	TB	12	4.67	0.917**
	Mets	13	4.66	
RDPE	TB	12	5.17	0.684**
	Mets	13	5.13	

L, lesional; PE, perilesional edema.  
The values are given as mean ± SD.  
MD, AD, RD are in Units of 10<sup>-3</sup> mm<sup>2</sup>/sec.  
\*\*Independent sample t test.

enhancement such as nodular or ring enhancement<sup>1,8,14</sup> and may mimic metastases, lymphomas, gliomas, and other infective granulomas. On DWI, both metastatic and tubercular lesions show variable signal intensity with noncontributing ADC values.<sup>8</sup>

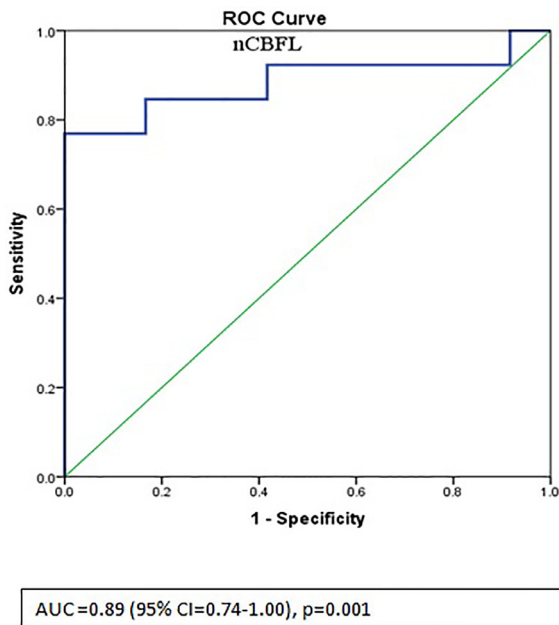


**FIG 5.** ROC curve showing AUC for normalized CBF from the enhancing portion of metastases.

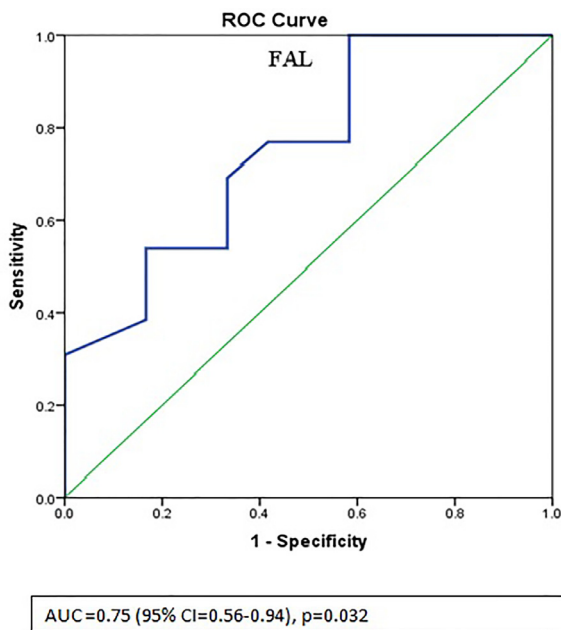


**FIG 6.** ROC curve showing AUC for FAL from the enhancing portion of tuberculomas.

ASL and DSC perfusion MRI studies have shown significantly lower perfusion values in the perilesional edema surrounding metastases than surrounding glioblastoma multiforme (GBM).<sup>15,16</sup> Several DSC perfusion studies have shown promising results in differentiating neoplastic from non-neoplastic lesions with very few studies on tubercular and metastases differentiation.<sup>8,9,17,18</sup> We have used ASL-perfusion MRI technique, because of its noninvasiveness and no contrast requirement which makes ASL safer to use in children, pregnant women, in patients with deranged renal function and for studies requiring regular follow-ups.

In this study, the comparison between metastases and tuberculoma showed statistically significant higher median nCBFL in metastatic lesions compared to tuberculoma while nCBF from perilesional edema comparison was statistically insignificant (Table 1).

Angiogenesis occurs in both neoplastic and non-neoplastic lesions, and the differences in the CBF is due to variable expression of vasoactive endothelial growth factor (VEGF), cytokines, and microvascular density which is more persistent in neoplastic lesions compared to non-neoplastic. In comparison to normal CWM, CBF values were more from lesion than perilesional edema. The low nCBFL value in the perilesional edema is due to vasoconstriction secondary to the raised interstitial pressure.<sup>15,19,20</sup>

Our study results agree with a retrospective DSC perfusion study in ring enhancing 34 tuberculomas and 10 metastases, which revealed peripheral hyperperfusion in tuberculomas ( $rCBV = 2.04 \pm 0.61$ ) and metastases ( $rCBV = 5.43 \pm 2.1$ ) while hypoperfused perilesional edema in both cases. Analysis of the values by ROC curve method revealed a cut-off value of  $\geq 3.745$  for differentiating ring-enhancing metastases from ring-enhancing tuberculomas.<sup>9</sup> A retrospective study in 22 patients of tuberculomas and metastases revealed significantly high rCBV in metastatic lesions ( $5.06 \pm 2.13$ ) and no significant difference in ADC (apparent diffusion coefficient).<sup>8</sup> We found higher median FAL in tuberculoma lesions than metastases ( $p = 0.031$ ) which points more toward the white matter microstructural destruction in metastases. The FA value is mainly affected by white matter fiber's diameter, density and contours and higher FA value indicates the more structured and regular orientation. No statistically significant difference was found in other DTI parameters. A DTI study in 24 subjects of metastases and high-grade gliomas showed no statistically significant difference in peritumoral FA measurement.<sup>21</sup>

A recent DTI study in 22 subjects of brain tuberculosis and toxoplasmosis revealed statistically significant difference in intralesional FA values while no significant difference in perilesional edema FA values.<sup>22</sup> No related study on DTI differentiating the tuberculomas from metastases has been found while searching the literature. Analysis of ROC curve of metastases showed higher AUC of nCBFL than that of FAL. These results suggest that addition of ASL compared to DTI may help in improved differentiation among these two closely mimicking lesions especially in the presence of contrast administration contraindication.

### Limitations

Our current study results are although encouraging, however, there were few limitations. (1) A small sample size. (2) No histopathological confirmation of brain lesions. However, histopathological confirmation in non-neoplastic lesions may be practically difficult and we suggest utility of more noninvasive imaging methods (ASL) to improve the reliability of our current findings. (3) Manual ROI placement. Study results might be biased due to manual ROI placement which usually affects all the ROI-based studies. (4) Inherent limitations of ASL technique. Echo planar imaging (EPI)-based ASL technique is associated with of low signal to noise ratio (SNR), lower temporal and spatial resolution and greater susceptibility artifacts. However, 3D PCASL (3T GE HDXT) is fast spin echo (FSE) based read-out and gives better SNR, fewer susceptibility artifacts and better labeling efficiency.<sup>23,24</sup>

### Conclusions

Despite these limitations, our study results suggest that a combined analysis of noninvasive ASL and DTI techniques can help in the differentiation of metastasis from tuberculomas which may have treatment implications. Our prior experience to ASL suggests that it can be useful in different pathologies at the expense of few minutes and being a noncontrast, it can be performed in any patient who is undergoing MR exam.<sup>7,23,25</sup>

### Acknowledgment

No financial disclosure.

## Supplementary materials

Supplementary material associated with this article can be found in the online version at <https://doi.org/10.1067/j.cpradiol.2018.09.003>.

## References

- Kim TK, Chang KH, Kim CJ, et al. Intracranial tuberculoma: Comparison of MR with pathologic findings. *AJNR Am J Neuroradiol* 1995;16:1903–8.
- Rock RB, Olin M, Baker CA, et al. Central nervous system tuberculosis: Pathogenesis and clinical aspects. *Clin Microbiol Rev* 2008;21:243–61.
- Posner JB. Management of brain metastases. *Rev Neurol* 1992;148:477–87.
- Idrish MN, Sokrab TE, Arbab MA, et al. Tuberculoma of the brain: a series of 16 cases treated with antituberculosis drugs. *Int J Tuberc Lung Dis* 2007;11:91–5.
- Nagar VA, Ye J, Xu M, et al. Multivoxel MR spectroscopic imaging—distinguishing intracranial tumours from non-neoplastic disease. *Ann Acad Med Singapore* 2007;36:309–13.
- Grade M, Tamames JH, Pizzini FB, et al. A neuroradiologist's guide to arterial spin labeling MRI in clinical practice. *Neuroradiology* 2015;57:1181–202.
- Soni N, Dhanota DPS, Kumar S, et al. Perfusion MR imaging of enhancing brain tumors: Comparison of arterial spin labeling technique with dynamic susceptibility contrast technique. *Neurol India* 2017;65:1046–52.
- Chatterjee S, Saini J, Kesavadas C, et al. Differentiation of tubercular infection and metastases presenting as ring enhancing lesion by diffusion and perfusion magnetic resonance imaging. *Neurorad* 2010;37:167–71.
- Sankhe S, Baheti A, Ihare A, et al. Perfusion magnetic resonance imaging characteristics of intracerebral tuberculomas and its role in differentiating tuberculomas from metastases. *Acta Radiol* 2013;54:307–12.
- Guo AC, MacFall JR, Provenzale JM. Multiple sclerosis: Diffusion tensor MR imaging for evaluation of normal-appearing white matter. *Radiology* 2002;222:729–36.
- Price SJ, Jena R, Burnet NG, et al. Predicting patterns of glioma recurrence using diffusion tensor imaging. *Eur Radiol* 2007;17:1675–84.
- Romano A, Ferrante M, Cipriani V, et al. Role of magnetic resonance tractography in the preoperative planning and intraoperative assessment of patients with intra-axial brain tumours. *Radiol Med* 2007;112:906–20.
- Long DM. Capillary ultrastructure in human metastatic brain tumors. *J Neurosurg* 1979;51:53–8.
- Bernaerts A, Vanhoenacker FM, Parizel PM, et al. Tuberculosis of the central nervous system: overview of neuroradiological findings. *Eur Radiol* 2003;13(8):1876–90.
- Law M, Cha S, Knopp EA, et al. High-grade glioma and solitary metastases: Differentiation by using perfusion and proton spectroscopic MR imaging. *Radiology* 2002;222:715–21.
- Thompson G, Mills SJ, Coope DJ, et al. Imaging biomarkers of angiogenesis and the microvascular environment in cerebral tumours. *Br J Radiol* 2011;84:S127–44.
- Haris M, Gupta RK, Singh A, et al. Differentiation of infective from neoplastic brain lesions by dynamic contrast-enhanced MRI. *Neuroradiology* 2008;50:531–40.
- Floriano VH, Torres US, Spotti AR, et al. The role of dynamic susceptibility contrast-enhanced perfusion MR imaging in differentiating between infectious and neoplastic focal brain lesions: Results from cohort of 100 consecutive patients. *PLoS One* 2013;8:e81509.
- Gupta RK, Haris M, Husain N, et al. Relative cerebral blood volume is a measure of angiogenesis in brain tuberculoma. *J Comput Assist Tomogr* 2007;31:335–41.
- Tateishi U. Vasoactive endothelial growth factor-related angiogenesis. *Radiology* 2005;235:191–9.
- Lu S, Ahn D, Johnson G, et al. Peritumoral diffusion tensor imaging of high-grade gliomas and metastatic brain tumors. *AJNR Am J Neuroradiol* 2003;24:937–41.
- Chu XL, Zhao LP, Ma JX, et al. Application of diffusion tensor imaging in AIDS patients with brain opportunistic diseases: A comparative study of tuberculosis and toxoplasmosis. *Radiol Infect Dis* 2015;2:11–5.
- Soni N, Jain A, Kumar S, et al. A prospective non-invasive arterial spin labeling magnetic resonance perfusion study to evaluate the Effects of age and gender on normal cerebral blood flow. *Neurol India* 2016;64:32–8.
- Soni N. Author's reply: Arterial spin labeling. *Neurol India* 2018;66:285.
- Soni N, Srindharan K, Kumar S, et al. Arterial spin labeling perfusion: Prospective MR imaging in differentiating neoplastic from non-neoplastic intra-axial brain lesions. *Neuroradiol J* 2018, <https://doi.org/10.1177/1971400918783058>. Jan 11971400918783058. [Epub ahead of print].